Petroleum Science 19 (2022) 1939–1949

Contents lists available at ScienceDirect

Petroleum Science

journal homepage: www.keaipublishing.com/en/journals/petroleum-science

Original Paper

Pore and fracture characteristics of Cretaceous tight reservoir and its control effect on hydrocarbon accumulation in the Liuhe Basin

Wen-Hao Li [a, b, *], Er-Qiang Yang [a, b], Min Wang [a, b], Yan-Ran Huang [c]

[a] Laboratory of Deep Oil and Gas, China University of Petroleum (East China), Qingdao, Shandong, 266580, China
[b] School of Geosciences, China University of Petroleum (East China), Qingdao, Shandong, 266580, China
[c] Hunan Provincial Key Laboratory of Shale Gas Resource Utilization, Hunan University of Science and Technology, Xiangtan, Hunan, 411201, China

ARTICLE INFO

Article history:
Received 14 September 2021
Received in revised form
5 March 2022
Accepted 16 June 2022
Available online 24 June 2022

Edited by Jie Hao

Keywords:
Tight reservoir
Microscopic pore structure
Microfracture
Porosity evolution
Hydrocarbon accumulation
the liuhe Basin

ABSTRACT

Tight oil and gas in the Cretaceous has been found in the Liuhe Basin, but the rules of tight reservoir and oil and gas accumulation are not clear. This paper discusses the developmental characteristics and evolution law of pores and fractures in the Cretaceous tight reservoir in the Liuhe Basin, and reveals its controlling effect on tight oil and gas accumulation. The results show that intercrystalline pores, intergranular pores and dissolution pores are scattered and only developed in shallow tight reservoirs, while microfractures are developed in both shallow and deep layers, which are the main type of reservoir space in the study area. The results of mercury intrusion porosimetry and nitrogen gas adsorption show that with the increase of depth, the proportion of macropores (microcracks) increases, while the proportion of micropores decreases. There are two stages of microfractures developed in the study area, corresponding to the initial fault depression stage from late Jurassic to early late Cretaceous and compressional uplift at the end of late Cretaceous. According to the principle of "inversion and back-stripping method", combined with the data of optical microscopy and inclusions, the time of each key diagenesis and its contribution to porosity are revealed, and the porosity evolution history of reservoirs in different diagenetic stages is quantitatively restored. The porosity reduction rate of compaction can reach more than 80%, which is the main reason for reservoir densification. The relationship between pore evolution history and oil and gas accumulation history reveals that during the oil and gas filling period of the Xiahuapidianzi Formation (90–85 Ma), the reservoir porosity is only 1.15%, but the development of microfractures in the first stage of the reservoir is conducive to oil and gas accumulation.

1. Introduction

With the increasing depletion of conventional oil and gas, tight oil and gas has become the most realistic replacement resource at present (Dai et al., 2012). Compared with conventional reservoir, tight reservoir has the characteristics of poor physical properties, strong heterogeneity and complex microscopic pore-throat systems (Feng et al., 2013; Qiao et al., 2019, 2020). Tight reservoir is characterized by micro or nano-sized pore throat while micro or centimeter-scale pore throat dominates in the conventional reservoir (Zou et al., 2015). Thus, microscopic pore structure of tight reservoir is an important factor which affects its reservoir performance and seepage capacity. It is of great significance to clarify the microscopic pore structure for understanding the enrichment mechanism of tight oil and gas. In recent years, research works have been focused on microscopic pore structure characteristics of tight reservoir through analysis of mercury intrusion porosimetry (MIP), nitrogen gas adsorption (N_2GA), field emission scanning electron microscopy (FE-SEM), nuclear magnetic resonance (NMR) and other methods (Schmitt et al., 2013; Anovitz and Cole, 2015; Li et al., 2016; Xiao et al., 2016; Zhang et al., 2017, 2020; Lai et al., 2018; Gao et al., 2019; Tian et al., 2019; Hu et al., 2020; Kong et al., 2020; Wang et al., 2021; Zhao et al., 2021). In addition, the natural fractures may be relatively developed in tight reservoir under the diagenesis and tectonic effects, which can be used as important reservoir space and infiltration channels for tight reservoir, and is of great significance for oil and gas accumulation (Nelson et al., 2000; Zeng and Li, 2009; Wang et al., 2020; Micheal

* Corresponding author.
E-mail address: liwh@upc.edu.cn (W.-H. Li).

https://doi.org/10.1016/j.petsci.2022.06.015

et al., 2021). The micro-nano pore-throat network system of tight reservoir is developed, capillary pressure limits the effect of buoyancy, oil and gas migration and accumulation are mainly due to the difference in pressure between source rock and reservoir. The oil and gas migration distance is generally short, which is mainly primary migration or short-distance secondary migration (Zou et al., 2009; Zhang et al., 2018). Therefore, the mechanism of oil and gas charging, migration and accumulation in the micro-nano pore-throat network system is the core scientific issue of the tight oil and gas accumulation mechanism.

Although there is only one exploration well (Well LC1) in the Liuhe Basin, outcrops show there are a large number of black-brown oils in the sandstone fractures of the Hengtongshan Formation and the Xiahuapidianzi Formation. However, there are no research work on the Cretaceous tight reservoir and oil and gas accumulation in the Liuhe Basin. Thus, this paper discusses the characteristics of micro-pore structure, fracture and porosity evolution of the Cretaceous tight reservoirs in the Liuhe Basin, and reveals the controlling effect of pore and fracture evolution on oil and gas accumulation.

2. Geological background

The Liuhe Basin, located between the Dunhua-Mishan fault and the Yalu River fault, is adjacent to the Huihua Basin in the north and the Tonghua Basin in the south. The basin consists of five parts, which are the western Slope Belt, the southern Xinbin Uplift, the Shengshui Depression, the Ankou Depression and the Xiangyang Depression (Fig. 1a and b) (Zhang et al., 2017; Xu et al., 2019). The Well LC1 is located between the Ankou Depression and the Shengshui Depression around the Hengtong Town, close to the Dunhua-Mishan fault (Fig. 1b). The base of the basin is Proterozoic metamorphic rocks, and the late Paleozoic, early Mesozoic strata are missing. The tectonic evolution of the basin is controlled by the activity of the Dunhua-Mishan fault. And the lacustrine facies and volcanic eruption facies are mainly developed in the Liuhe Basin. The basin experienced the early initial fault depression period from late Jurassic to late Cretaceous, extruding and uplifting stage at the end of the late Cretaceous, and the uplift and denudation in the Paleogene, resulting in the formation of continental volcanic sedimentary basin (Wang et al., 2020).

Above the base, there are the Jurassic Houjiatun Formation, the Cretaceous Lamenzi Formation, Dashatan Formation, Baodaqiao Formation, Xiahuapidianzi Formation, Hengtongshan Formation and Heiwaizi Formation, and the Paleogene Meihe Formation (Fig. 2). Purple siltstone intercalated with yellow-green argillaceous siltstone, black siltstone and carbonaceous shale are mainly developed in the Houjiatun Formation. Andesite, tuffaceous sandstone, gray conglomerate, sandstone and siltstone are deposited in the Lamenzi Formation. The lithology of the Dashatan Formation mainly includes grayish green and white thin gravel sandstone, siltstone and shale. Grayish green and yellowish green tuffaceous fine sandstone and siltstone with local tuff are mainly developed in the Baodaqiao Formation. Yellow, gray siltstone, carbonaceous shale, sandstone intercalated with coal seam are developed in the Xiahuapidianzi Formation. The Hengtongshan Formation is mainly composed of tuffaceous conglomerate, sandstone and shale, intercalated with coal seam. The Heiwaizi Formation is mainly composed of red, purple, variegated conglomerate and interbedded sandstone and siltstone, while the Meihe Formation develops gray glutenite, gray-black mudstone and shale (Fig. 2). The Mesozoic hydrocarbon source rocks in the basin are the Lower Cretaceous Dashatan Formation, Xiahuapidianzi Formation and Hengtongshan Formation, among which the gray-black mudstone of the Xiahuapidianzi Formation has the best hydrocarbon potential, with an average TOC of 1.37% (Xu et al., 2019). Clastic rocks, volcanic rocks and pyroclastic rocks of the Cretaceous Lamenzi Formation, Dashatan Formation, Baodaqiao Formation, Xiahuapidianzi Formation and Hengtongshan Formation may be explored as reservoirs. Generally, it is characterized as a typical tight reservoir by ultra-low porosity and ultra-low permeability (Xu et al., 2019).

3. Quantitative characterization of reservoir space

3.1. Type of reservoir space

Optical microscopy and SEM revealed that the Cretaceous reservoir in the Liuhe Basin was tight and the pores are sporadic. Calcite intergranular pores (Fig. 3a), clay mineral intergranular pores (Fig. 3b), and solution pores formed by weak dissolution of

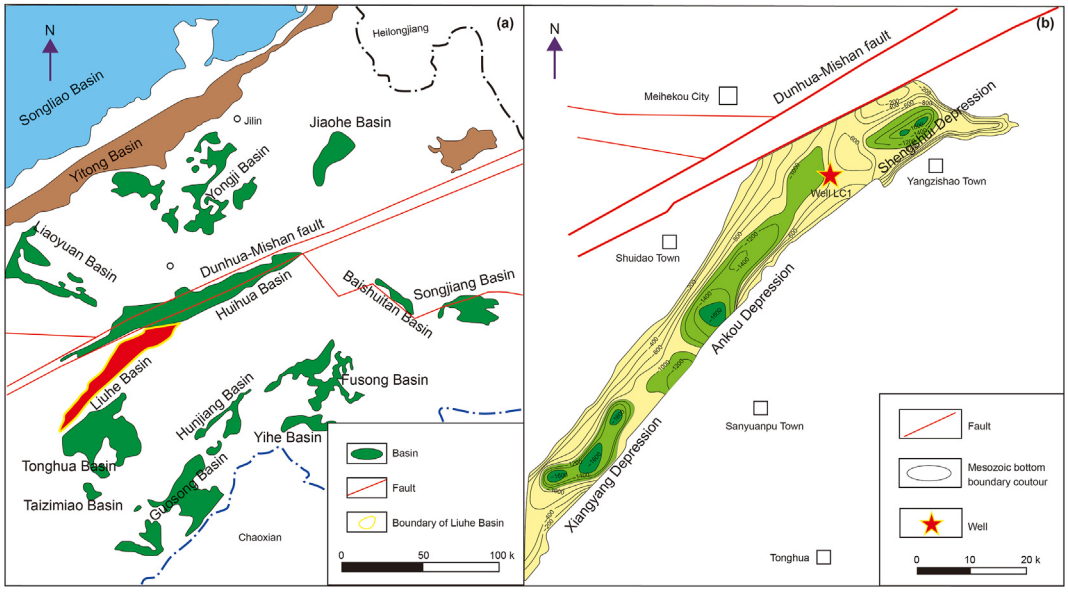

Fig. 1. (a) Tectonic division of the Liuhe Basin; (b) Structural map of Well LC1.

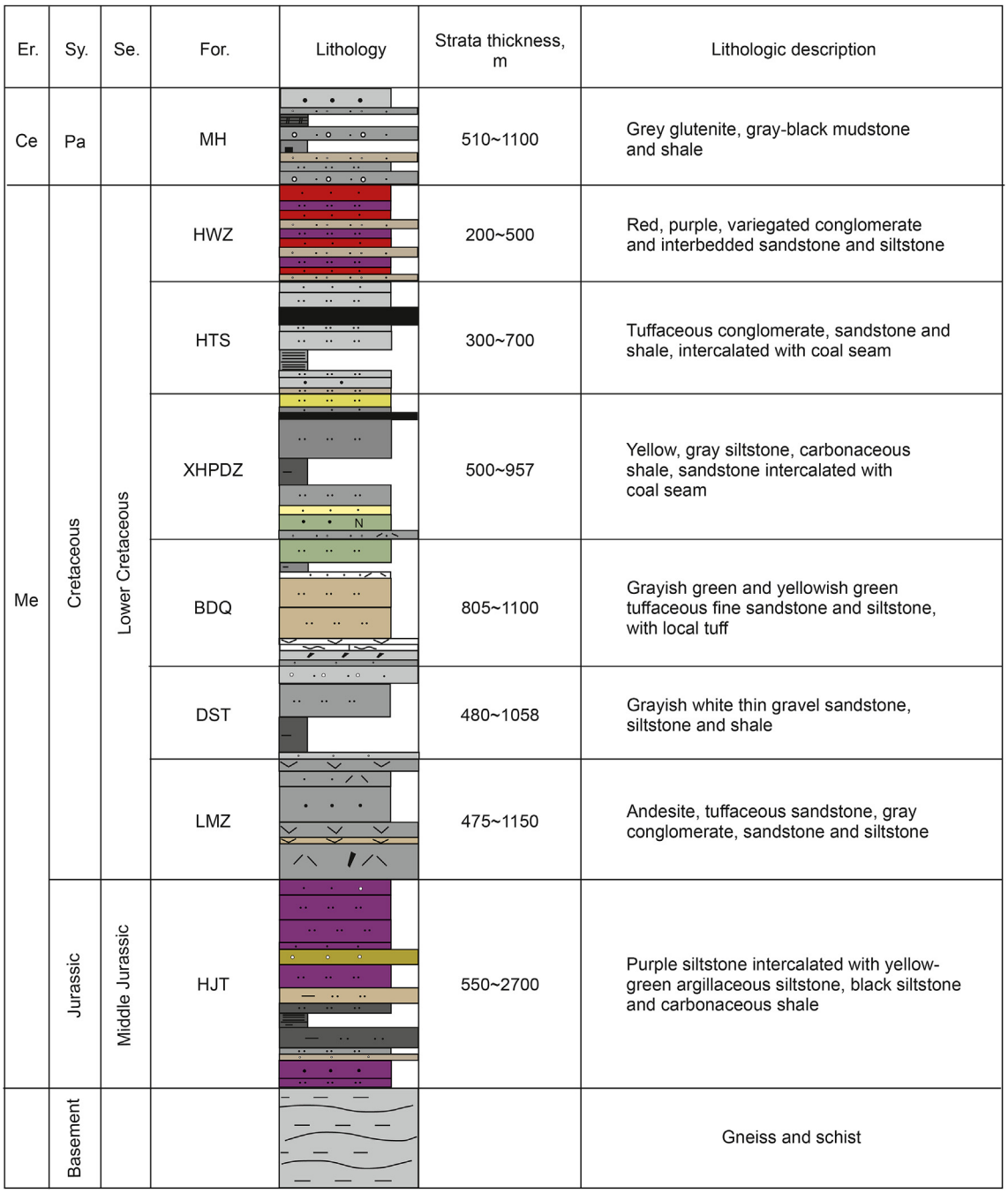

Fig. 2. Generalized stratigraphy of the Liuhe Basin. Er, Erathem; Sy, System; SE, Series; For, Formation; Ce, Cenozoic; Me, Mesozoic; Pa, Paleogene; MH, Meihei Formation; HWZ, Heiwaizi Formation; HTS, Hetongshan Formation; XHPDZ, Xiahuapidianzi Formation; BDQ, Baodaoqiao Formation; DST, Dashatan Formation; LMZ, Lamenzi Formation; HJT, Houjiatun Formation.

feldspar can be observed under microscope (Fig. 3c). However, the pores are mainly developed in the shallow layer with a buried depth of less than 1000 m, and most of the pores are filled with cements (Fig. 3). Microfractures are commonly distributed in both shallow and deeper layers, and are the main type of reservoir space in this area, which can be further divided into structural fractures (Fig. 3d) and diagenetic fractures (Fig. 3e and f). These microfractures are often filled with asphalt (Fig. 3d, e, f), which suggest that the development and distribution of microfractures may control the oil and gas distribution in the study area.

3.2. Quantitative characterization of reservoir space

3.2.1. MIP analysis

AutoPore IV 9500 porosimeter was used to carry out the MIP experiment. Before analysis, samples should be dried in a vacuum oven for 1 h with the temperature 150 °C, and details were reported in Li et al. (2017). According to the results of MIP, the percentage of pore throat in the range of 10–100 μm, 1–10 μm (super-capillary pores), 0.1–1 μm (capillary pores), 0.01–0.1 μm (micro-capillary pores) and less than 0.01 μm (nano-capillary pores) were calculated respectively, and the variation law between pore throat and depth

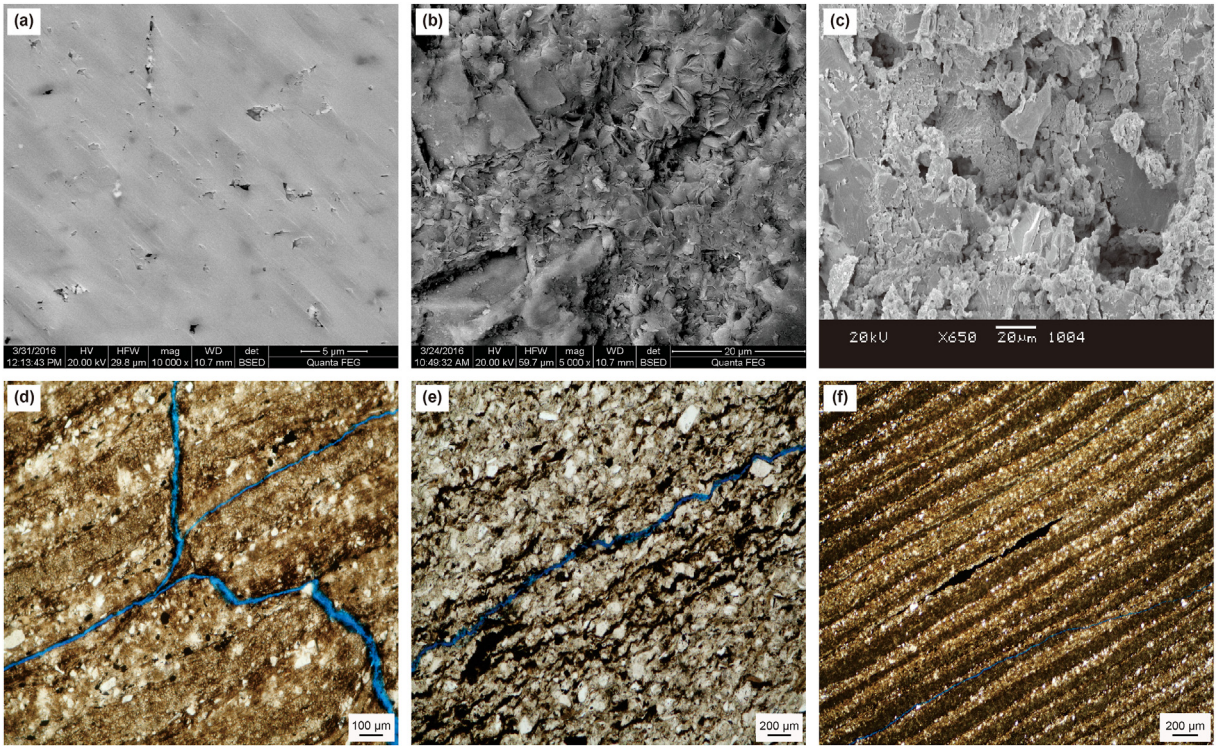

Fig. 3. Types of reservoir space of Cretaceous tight reservoir in the Liuhe Basin. (a) Well LC1, 754 m, Xiahuapidianzi Formation, gray glutenite, calcite intercrystalline pores; (b) LC1, 400 m, Hengtongshan Formation, silty mudstone, clay mineral intergranular pores; (c) Well LC1, 790 m, Xiahuapidianzi Formation, tuff, feldspar solution pores; (d) Well LC1, 1237 m, Xiahuapidianzi Formation, silty dolomitic mudstone, "trigeminal fracture"; (e) Well LC1, 825 m, Xiahuapidianzi Formation, argillaceous siltstone, diagenetic fracture; (f) Well LC1, 1237 m, Xiahuapidianzi Formation, silty dolomitic mudstone, diagenetic fracture.

was discussed (Fig. 4). The results show that the proportion of pores with throat radius of 10–100 μm and 1–10 μm is less than 10%, and the change is not obvious with the increase of depth (Fig. 4). The proportion of pores with throat radius between 0.1–1 μm and 0.01–0.1 μm increased significantly with the increase of burial depth, while the pores with throat radius less than 0.01 μm sharply decreased with the increase of burial depth (Fig. 4). The above results show that with the increase of depth, the proportion of macropores increases gradually, while the proportion of micropores decreases gradually. Combined with the analysis results of reservoir space types, it is revealed that with the increase of buried depth, the proportion of macropores or microfractures in total pores increases gradually. Due to the influence of compaction, the pore size of micropores decreases sharply when the burial depth increases, so the proportion of micropores decreases obviously.

3.2.2. N2GA analysis

ASAP2460 automatic surface area and pore size analyzer is used to carry out the N2GA experiment. Before analysis, samples should be smashed to 40–80 mesh and dried for 6 h with the temperature 110 °C, and details were listed in Tian et al. (2019). The shape of the adsorption curve can qualitatively evaluate the pore size distribution of tight rocks. Based on the classification of deBoer hysteresis loops, IUPAC recommended a new classification standard, which divided hysteresis loops into four categories: H1, H2, H3 and H4. The pore throat shapes of the corresponding adsorbents are

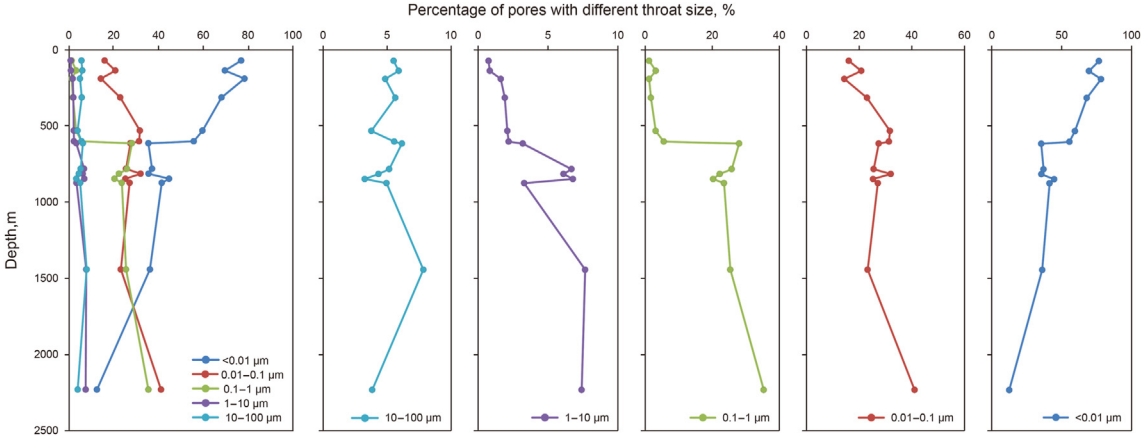

Fig. 4. The relationship between percentage of pores with different throat size and depth.

cylindrical holes with openings at both ends (type H1), "ink bottle" shaped pores with thin openings and wide bodies (type H2), slit pores with parallel plate structure (type H3) and slit pores with conical structure (type H4), respectively (Sing et al., 1985). With the increase of burial depth, the pore shapes gradually change from H2 to H3 (Fig. 5), which is from the "ink bottle" shaped pores with thin openings and wide bodies to the slit pores of parallel plate structure (Wang et al., 2010; Janssen et al., 2011). As can be seen from the results of reservoir space types, pores can hardly be detected in tight reservoirs with buried depths greater than 1000 m in the study area, while fractures are developed in both shallow and deep layers. Therefore, it can be considered that the slit pores mentioned above were microfratures. Among them, two samples with depths of 70 m and 313 m (Fig. 5a and b) are typical "link bottle" pores. While samples with depths of 1146.6 m and 1385.1 m (Fig. 5c and d) are transitional or partial microfractured type (mainly micro-fractures, with a small amount of "ink bottle" pores). And two samples of 1745 m and 2458 m (Fig. 5e and f) represente the microfractured type. With the increase of depth, the proportion of mesoporous pores decreases gradually, while the proportion of macropores gradually increases (Fig. 6), that is, the proportion of microfractures in total pores gradually increases, which is consistent with the results of MIP.

4. Evolution characteristics of fracture and porosity

4.1. Fracture evolution sequence

The Liuhe Basin has experienced two stages of tectonic movement: the initial faulting stage from late Jurassic to early stage of late Cretaceous and the compressional uplift stage from late Cretaceous. Therefore, two stages of tectonic fractures have been formed correspondingly. The evolution sequence of micro-fractures in this area was determined by microscopic thin section observation, combined with the analysis of the intersecting relationship between micro-fractures and mineral intersection and dissolution-filling (Fig. 7a–d). The evolution sequence is described below: tectonic fracture in the first stage → weak dissolution → asphalt or carbonate mineral filling →tectonic fracture in the second stage. From the above analysis, it can be seen that as the buried depth increases, the proportion of micro-fractures in the total pores in tight reservoirs gradually increases. Areal porosity of the micro-fracture is calculated with the results of most samples in the range from 0.5% to 2.5% (Fig. 8). Areal porosity of the micro-fracture also gradually increases with the increase of burial depth (Fig. 8).

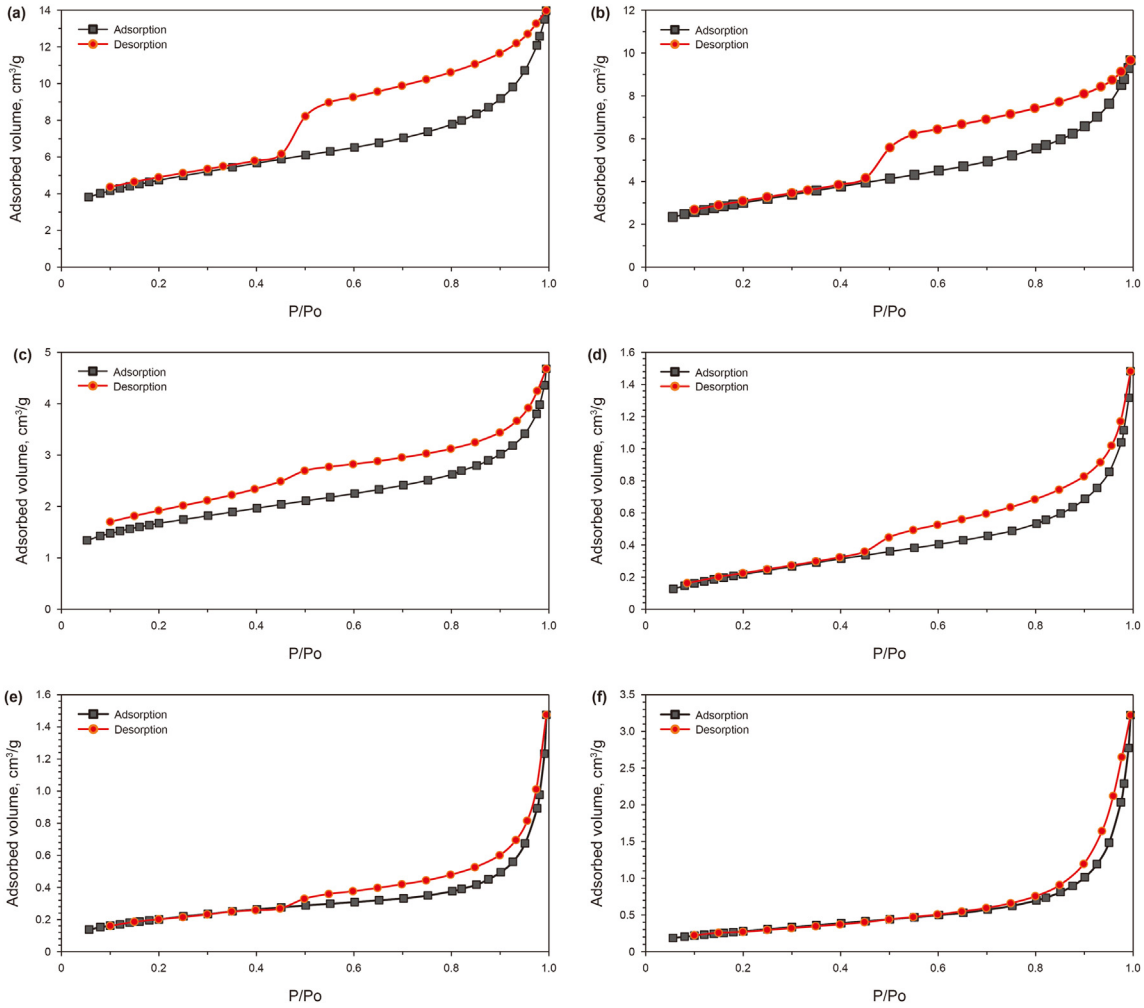

Fig. 5. Nitrogen adsorption-analytical curve of tight reservoir samples at low temperature. (a) Well LC1, 70 m, Hengtongshan Formation, dark gray mudstone; (b) Well LC1, 313 m, Hengtongshan Formation, tuffaceous breccia; (c) Well LC1, 1146.6 m, Xiahuapidianzi Formation, tuffaceous mudstone; (d) Well LC1, 1385.1 m, Xiahuapidianzi Formation, dark gray medium sandstone; (e) Well LC1, 1745 m, Baodaqiao Formation, gray porphyry; (f) Well LC1, 2458 m, basement, dark gray tuff.

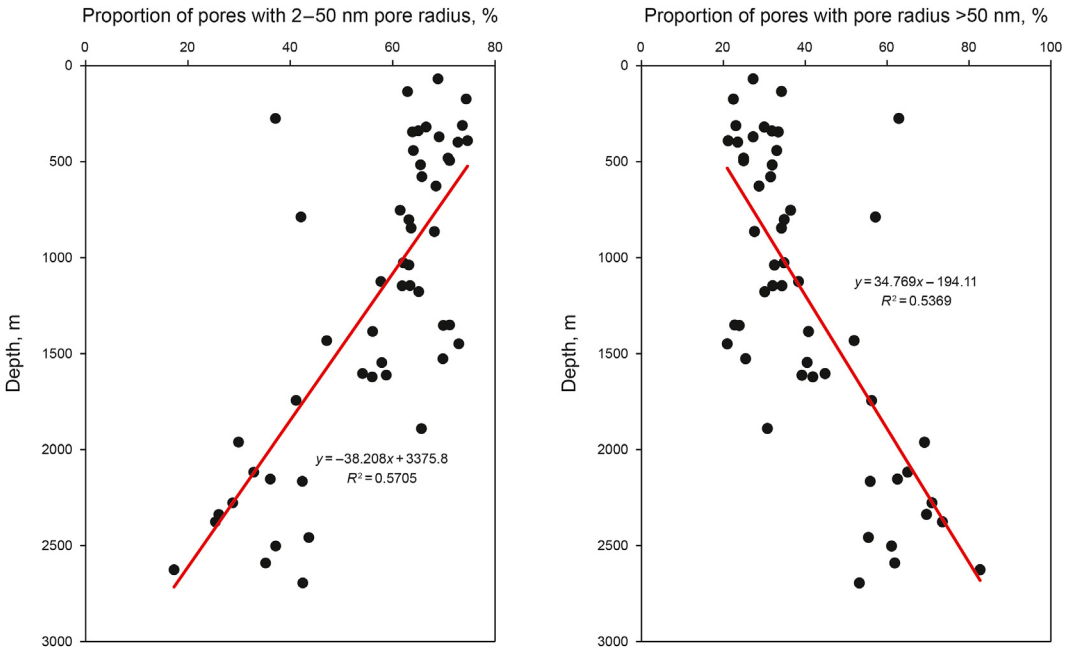

Fig. 6. The relationship between the proportion of mesoporous pores and macropores and depth.

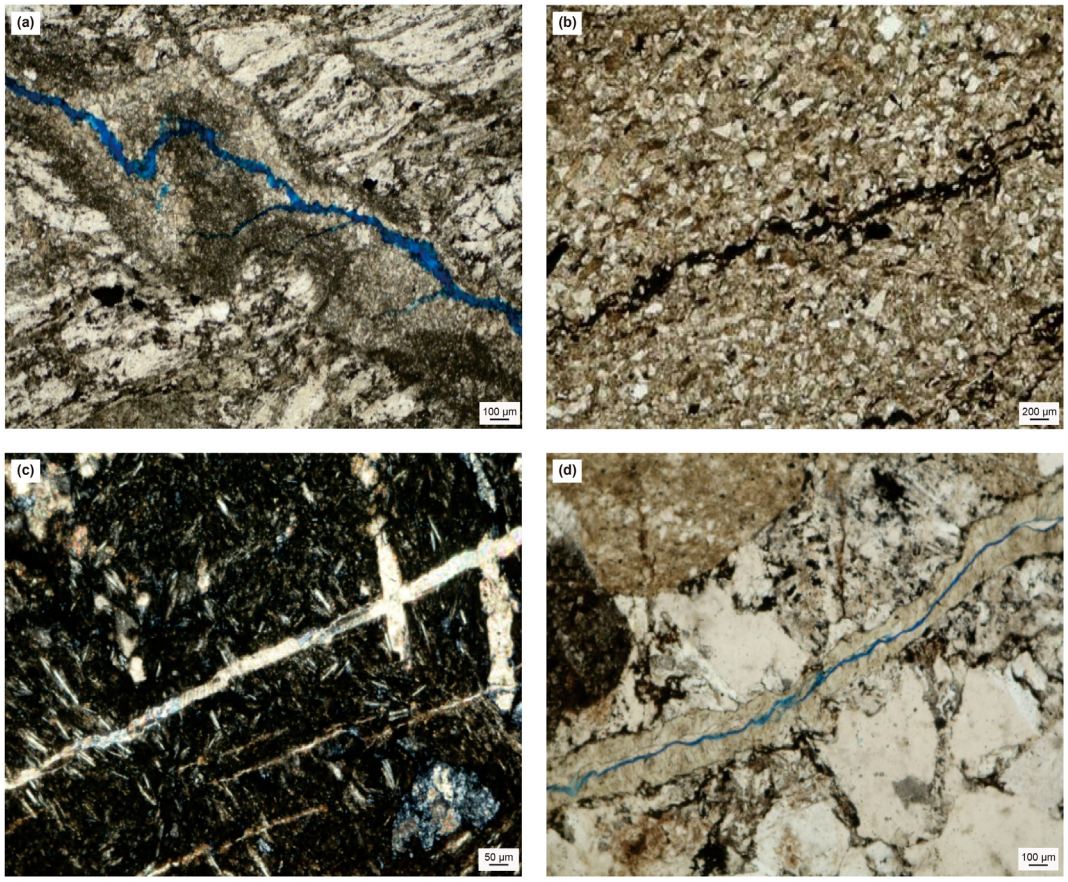

Fig. 7. The evolution sequence of micro-fractures. (a) Well LC1, 1846 m, Baodaqiao Formation, felsic mylonite, dissolution fracture associated with tectonic movement; (b) Well LC1, 825 m, Xiahuapidianzi Formation, argillaceous siltstone, bitumen filled in fractures; (c) Well LC1, 815 m, Xiahuapidianzi Formation, trachyandesite, fracture filled by calcite; (d) Well LC1, 1528 m, Xiahuapidianzi Formation, feldspar lithic sandstone, the second tectonic fracture formed above the fillings in the first tectonic fracture.

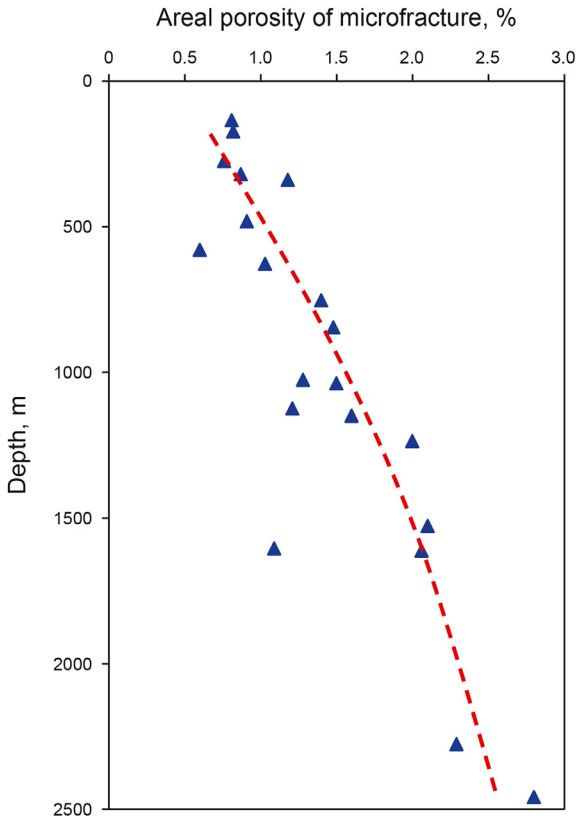

Fig. 8. The relationship between areal porosity of microfracture of the tight reservoir and depth.

4.2. Evolution characteristics of porosity

In order to illustrate the characteristics of porosity evolution, it is necessary to clarify the diagenetic evolution sequence. Through a large number of optical microscope observation, the contact relationship between authigenic minerals and various pores was analyzed (Fig. 9a–d), and the evolution sequence of reservoir diagenesis was established: Compaction→ Dissolution of feldspar or debris→ Carbonate cementation→ Pyrite metasomatism. The evolution sequence is mainly due to the following phenomenon: (1) The dissolution residue of feldspar can be observed, and the dissolution pores are filled with calcite, indicating that carbonate cementation occurred after dissolution. (2) Since the agglomerated and cubic pyrites replace the carbonate cements, it can be inferred that the metasomatism period of the pyrites is later than the formation time of the carbonate cements. According to the data of inclusions, the time of dissolution and cementation can be determined. The Xiahuapidianzi Formation, for example, began to deposit in 122 Ma, when the lowest homogenization temperature of quartz inclusions is 81 °C. According to the corresponding time of thermal history, 111 Ma is considered to be the beginning of dissolution. The lowest temperature of calcite inclusions is 91 °C. According to the thermal history, the corresponding time is 108 Ma, which is considered to be the beginning of carbonate cementation, and the highest temperature of calcite inclusions is 110 °C. According to the thermal history, the corresponding time is 97 Ma, corresponding to the end of carbonate cementation.

Under the constraint of diagenetic evolution, the variation of reservoir porosity caused by different diagenetic events was obtained by using human-computer interactive image analysis technology, and the inversion stripping method was used to restore the reservoir porosity of the main diagenetic stages in the geological history period (Xi et al., 2015a, b; Ma et al., 2015; Wang et al., 2018; Teillet et al., 2019). Among them, the original porosity was mainly affected by particle sorting, and the original porosity of the reservoir sample can be obtained according to the particle size data. The reduced porosity of cementation and the increased porosity of dissolution can be obtained according to the area porosity method. The pore reduction of compaction was restored by inversion stripping method.

As compaction runs through the whole diagenesis, the compaction pore reduction should be allocated to each diagenetic stage reasonably according to correction rules. Taking the samples of the Xiahuapidianzi Formation at 1139 m as an example, the porosity evolution characteristics are shown in Fig. 10. The compaction ratio can quantitatively describe the strength of compaction, and the cementation porosity is a parameter that reflects the influence of cementation on the original pore space volume. The compaction porosity reduction rate of the study area is basically more than 80% (Fig. 11), and the cementation porosity reduction rate is in the range from 5.4% to 26.3%. Thus, compaction is the main reason for reservoir densification in the study area.

5. The process of tight oil and gas accumulation

Xiahuapidianzi Formation is taken as an example to discuss the tight oil and gas accumulation rules. There was light oil in the microfractures of the samples from the Xiahuapidianzi Formation, showing strong yellow-green and green fluorescence. Most of the inclusions are distributed in lines or belts along the microfractures that cut through the tuff quartz crystal fragments, with very low development abundance (GOI < 1%), and they are all natural gas inclusions and hydrocarbon-bearing brine inclusions (Fig. 12). The homogenization temperature of the brine inclusions associated with hydrocarbon fluid inclusions can reflect the hydrocarbon accumulation period. The oil and gas charging period of the Xiahuapidianzi Formation was in the middle and late Late Cretaceous (90–85 Ma) according to the distribution characteristics of the homogenization temperature of the inclusions, combining with the thermal history and burial history of the study area. At that time, the Xiahuapidianzi Formation source rocks were in the mature stage and had entered the period of a large amount of hydrocarbon generation (97–70 Ma). The reservoir was affected by strong compaction, and the porosity reduction effect was obvious, which makes the physical property poor. The porosity of the reservoir was only 1.15% during oil and gas charging period (Fig. 13). However, the development of microfractures in the first stage of the reservoir (before 90 Ma) is conducive to oil and gas accumulation. It can be observed under the microscope that the fractures in the Xiahuapidianzi Formation are filled with asphalt more commonly (Fig. 14), indicating that micro-fractures are the main type of storage space in the study area. The formation and evolution of the fractures have obvious control effect on oil and gas charging. The caprock was formed at 94 Ma, with good sealing properties, and was less affected by the late structure (70 Ma to present). Therefore, the hydrocarbon accumulation process of the Xiahuapidianzi Formation can be summarized as: the source rocks of the Xiahuapidianzi Formation began to form a large amount of oil and gas in the early Late Cretaceous, and accumulated in the microfractures of the Xiahuapidianzi Formation reservoirs.

6. Conclusions

The pores of the Cretaceous tight reservoirs in the Liuhe Basin are scattered, and only a small amount of calcite intercrystalline pores, clay mineral intergranular pores and feldspar dissolution

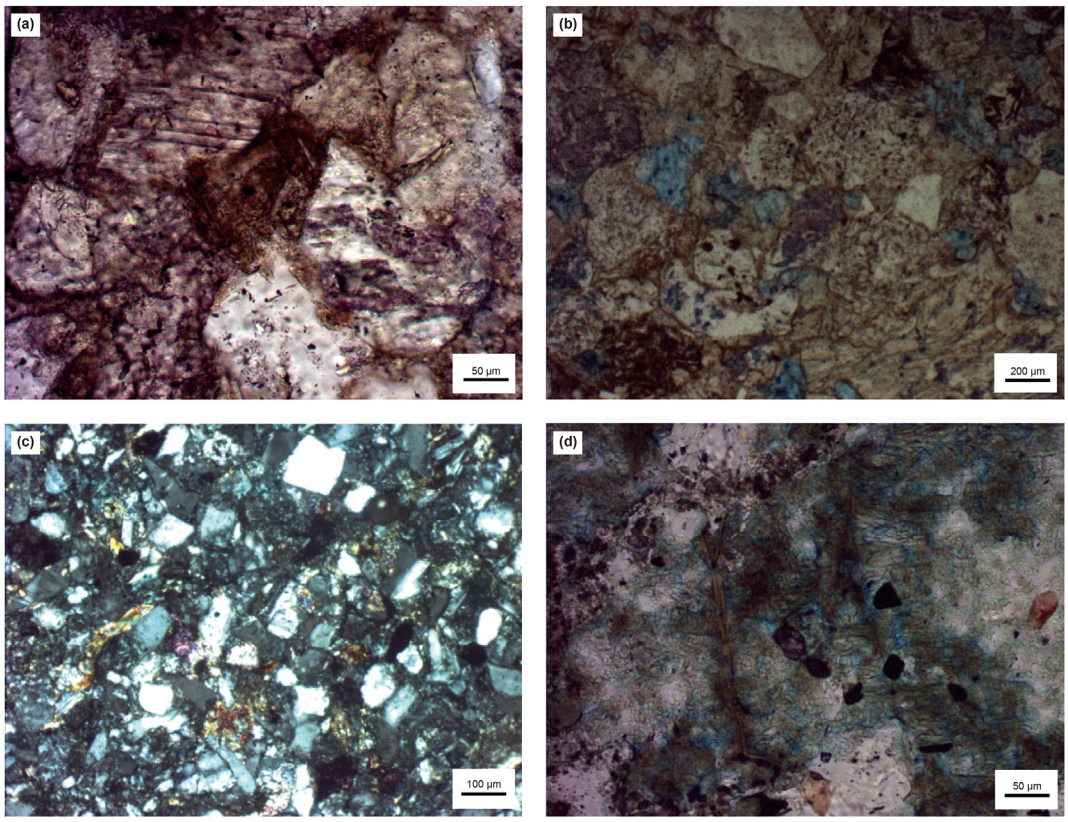

Fig. 9. Characteristics of diagenetic evolution sequence of the tight reservoir. (a) Well LC1, 321 m, Hengtongshan Formation, gray medium-sandstone, dissolution pores cemented by calcite; (b) Well LC1, 542 m, Hengtongshan Formation, gray fine sandstone, ferrodolomite metasomatism; (c) Well LC1, 1027 m, Xiahuapidianzi Formation, dark gray tuff, bent deformed mica; (d) Well LC1, 276 m, Hengtongshan Formation, dark gray tuff, ferrodolomite replaced by pyrite.

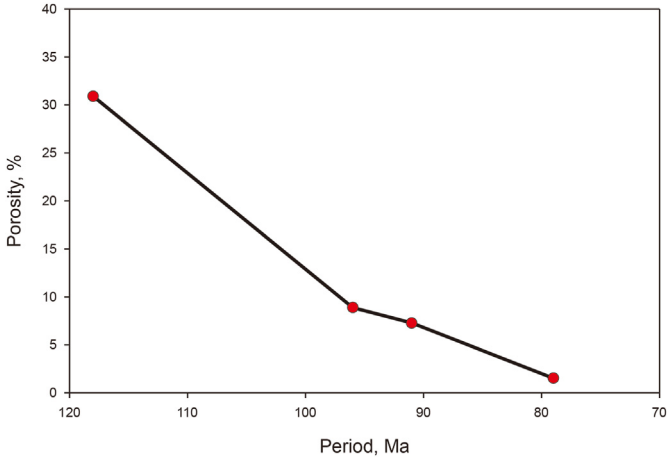

Fig. 10. Porosity evolution characteristics of the Xiahuapidianzi Formation.

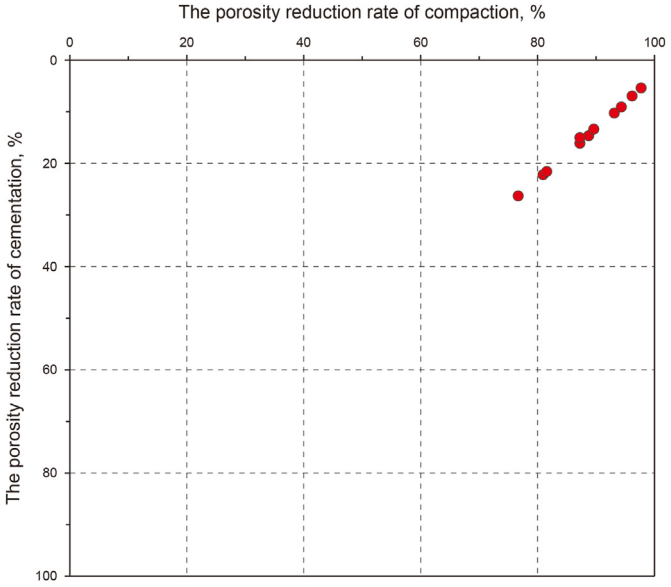

Fig. 11. Porosity reduction effect on compaction and cementation of the tight reservoir.

pores are developed in the shallow layers with the buried depth less than 1000 m. The type of reservoir space is mainly micro-fracture, which is distributed in both shallow and deep tight reservoirs. Two stages of microfracture formed related to the two stages of tectonic movement. With the increase of depth, the proportion of micropores in tight reservoir gradually decreases, while the proportion of microfractures in total pores gradually increases, and the areal porosity of the micro-fracture also increases.

The quantitative study of reservoir porosity evolution shows that porosity reduction rate of the compaction is more than 80%, which is the main factor causing the tight reservoir densified in the study area. The matching relationship between pore evolution history and hydrocarbon accumulation history reveals that during the oil and gas filling period of the Xiahuapidianzi Formation (90–85 Ma), the reservoir porosity is only 1.15%, but the

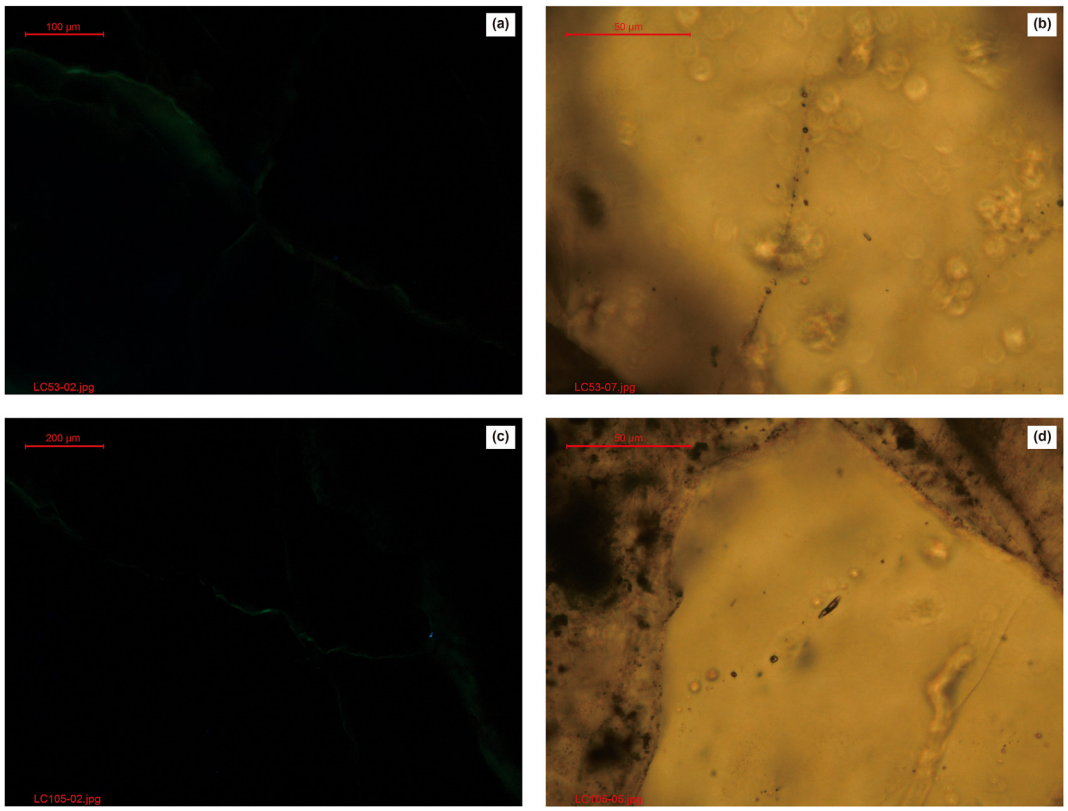

Fig. 12. The pictures showing characteristics of natural gas inclusions in the tight reservoir of the Xiahuapidianzi Formation.

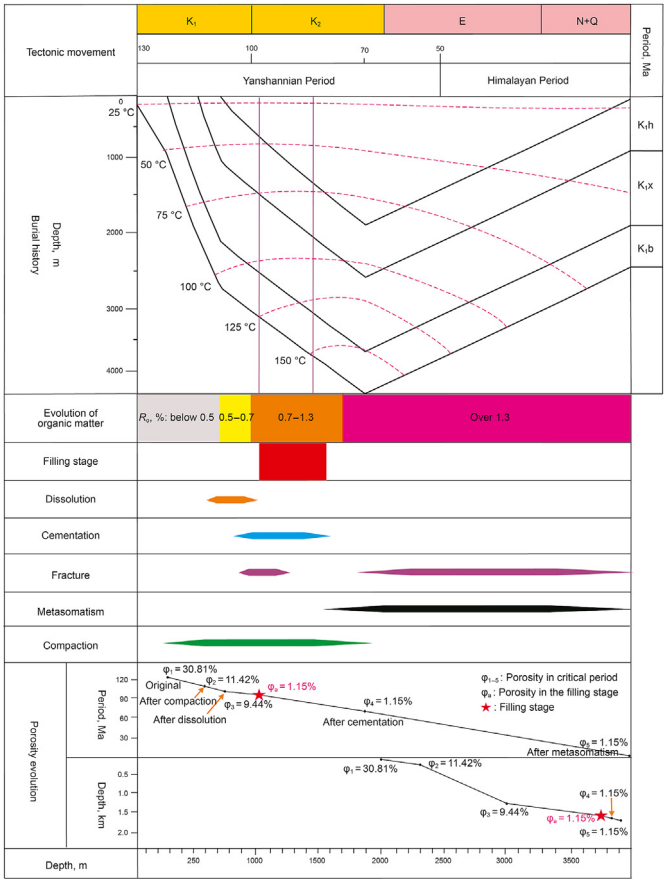

Fig. 13. The profile showing hydrocarbon accumulation process.

development of microfractures in the first stage of the reservoir is conducive to oil and gas accumulation.

Authors' contributions

All authors contributed to the study conception and design. The first draft of the manuscript was written by Wen-Hao Li. Conceptualization and methodology were performed by Wen-Hao Li and Er-Qiang Yang. Material preparation and data collection were performed by Min Wang and Yan-Ran Huang. All authors commented on the previous versions of the manuscript and approved the final manuscript.

Availability of data and material

Detailed information describing the experimental data is in the main text.

Declaration of competing interest

We confirm that there are no known conflicts of interest associated with this publication and there has been no significant financial support for this work that could have influenced its outcome. We confirm that the manuscript has been read and approved by all named authors and that there are no other persons who satisfied the criteria for authorship but are not listed. We further confirm that the order of authors listed in the manuscript has been approved by all of us. We confirm that we have given due consideration to the protection of intellectual property associated with this work and that there are no impediments to publication, including the timing of publication, with respect to intellectual property. In so doing we confirm that we have

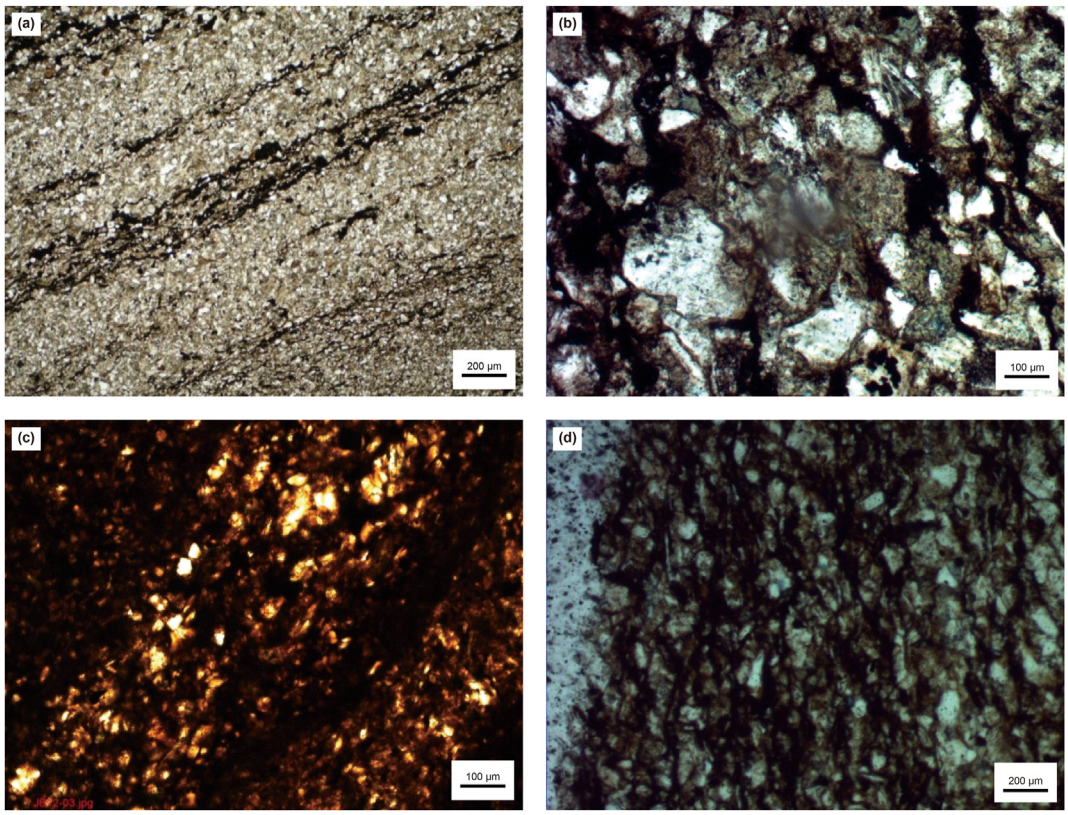

Fig. 14. Pictures showing bitumen distribution characteristics in the tight reservoir of the Xiahuapidianzi Formation. (a) Well LC1, 825 m, Xiahuapidianzi Formation, argillaceous siltstone; (b) Well LC1, 1139 m, Xiahuapidianzi Formation, dark gray tuffaceous sandstone; (c) Well LC1, 1354 m, Xiahuapidianzi Formation, argillaceous siltstone; (d) Well LC1, 1527 m, Xiahuapidianzi Formation, dark fine sandstone.

followed the regulations of our institutions concerning intellectual property.

Acknowledgements

This study was founded by the National Natural Science Foundation of China (41922015).

References

Anovitz, L.M., Cole, D.R., 2015. Characterization and analysis of porosity and pore structures. Rev. Mineral. Geochem. 80, 61–164. https://doi.org/10.2138/rmg.2015.80.04.

Dai, J.X., Ni, Y.Y., Wu, X.Q., 2012. Tight gas in China and its significance in exploration and exploitation. Petrol. Explor. Dev. 39, 277–284. https://doi.org/10.1016/S1876-3804(12)60043-3.

Feng, Z.H., Yin, C.H., Lu, J.M., Zhu, Y.K., 2013. Formation and accumulation of tight sandy conglomerate gas: a case from the Lower Cretaceous Yingcheng Formation of Xujiaweizi fault depression, Songliao Basin. Petrol. Explor. Dev. 40, 696–703. https://doi.org/10.1016/S1876-3804(13)60094-4.

Gao, Z.Y., Yang, X.B., Hu, C.H., Wei, L., Jiang, Z.X., Yang, S., Fan, Y.P., Xue, Z.X., Yu, H., 2019. Characterizing the pore structure of low permeability Eocene Liushagang Formation reservoir rocks from Beibuwan Basin in northern South China Sea. Mar. Petrol. Geol. 99, 107–121. https://doi.org/10.1016/j.marpetgeo.2018.10.005.

Hu, Q.H., Quintero, R.P., El-Sobky, H.F., Kang, J.H., Zhang, T., 2020. Coupled nanopetrophysical and organic-geochemical study of the Wolfberry play in Howard County, Texas U.S.A. Mar. Petrol. Geol. 122, 104663. https://doi.org/10.1016/j.marpetgeo.2020.104663.

Janssen, C., Wirth, R., Reinicke, A., Rybacki, E., Naumann, R., Wenk, H.R., Dresen, G., 2011. Nanoscale porosity in SAFOD core samples (San Andreas fault). Earth Planet Sci. Lett. 201, 179–189. https://doi.org/10.1016/j.epsl.2010.10.040.

Kong, X.X., Xiao, D.S., Jiang, S., Lu, S.F., Sun, B., Wang, J.M., 2020. Application of the combination of high-pressure mercury injection and nuclear magnetic resonance to the classification and evaluation of tight sandstone reservoirs: a case study of the Linxing Block in the Ordos Basin. Nat. Gas. Ind. B 7, 433–442. https://doi.org/10.1016/j.ngib.2020.09.001.

Lai, J., Wang, G.W., Wang, Z.Y., Chen, J., Pang, X.J., Wang, S.C., Zhou, Z.L., He, Z.B., Qin, Z.Q., Fan, X.Q., 2018. A review on pore structure characterization in tight sandstones. Earth Sci. Rev. 177, 436–457. https://doi.org/10.1016/j.earscirev.2017.12.003.

Li, W.H., Lu, S.F., Xue, H.T., Zhang, P.F., Hu, Y., 2016. Microscopic pore structure in shale reservoir in the argillaceous dolomite from the Jianghan Basin. Fuel 181, 1041–1049. https://doi.org/10.1016/j.fuel.2016.04.140.

Li, W.H., Wang, W.M., Lu, S.F., Xue, H.T., 2017. Quantitative characterization on shale-hosted oil reservoir: a case study of argillaceous dolomite reservoir in the Jianghan Basin. Fuel 206, 690–700. https://doi.org/10.1016/j.fuel.2017.06.056.

Ma, B.B., Cao, Y.C., Wang, Y.Z., Zhang, S.M., Jia, Y.C., 2015. Diagenetic evolution and its effect on reservoir-quality of fan delta sandstones during progressive burial: evidence from the upper part of the fourth member of Shahejie formation, Bonan sag, Jiyang depression. J. Cent. S. Univ. 22, 3042–3058. https://doi.org/10.1007/s11771-015-2841-y.

Micheal, M., Xu, W.L., Xu, H.Y., Zhang, J.N., Jin, H.J., Yu, H., Wu, H.A., 2021. Multi-scale modelling of gas transport and production evaluation in shale reservoir considering crisscrossing fractures. J. Nat. Gas Sci. Eng. 95, 104156. https://doi.org/10.1016/j.jngse.2021.104156.

Nelson, R.A., Moldovanyi, E.P., Matcek, C.C., Azpiritxaga, I., Bueno, E., 2000. Production characteristics of the fractured reservoirs of the La Paz field, Maracaibo basin, Venezuela. AAPG (Am. Assoc. Pet. Geol.) Bull. 84, 1791–1809. https://doi.org/10.1306/8626C393-173B-11D7-8645000102C1865D.

Qiao, J.C., Zeng, J.H., Jiang, S., Feng, S., Feng, X., Guo, Z., Teng, J.L., 2019. Heterogeneity of reservoir quality and gas accumulation in tight sandstone reservoirs revealed by pore structure characterization and physical simulation. Fuel 253, 1300–1316. https://doi.org/10.1016/j.fuel.2019.05.112.

Qiao, J.C., Zeng, J.H., Jiang, S., Wang, Y.N., 2020. Impacts of sedimentology and diagenesis on pore structure and reservoir quality in tight oil sandstone reservoirs: implications for macroscopic and microscopic heterogeneities. Mar. Petrol. Geol. 111, 279–300. https://doi.org/10.1016/j.marpetgeo.2019.08.008.

Schmitt, M., Fernandes, C.P., da Cunha Neto, J.A.B., Wolf, F.G., dos Santos, V.S.S., 2013. Characterization of pore systems in seal rocks using nitrogen gas adsorption combined with mercury injection capillary pressure techniques. Mar. Petrol. Geol. 39, 138–149. https://doi.org/10.1016/j.marpetgeo.2012.09.001.

Sing, K.S.W., Everett, D.H., Haul, R.A.W., Moscou, L., Pierotti, R.A., Rouquérol, J., Siemieniewska, T., 1985. Reporting physisorption data for gas/solid systems with special reference to the determination of surface area and porosity. Pure Appl. Chem. 57, 603–619. https://doi.org/10.1351/pac198557040603.

Teillet, T., Fournier, F., Gisquet, F., Montaggioni, L.F., Borgomano, J., Villeneuve, Q., Hong, F., 2019. Diagenetic history and porosity evolution of an Early Miocene

carbonate buildup (Upper Burman Limestone), Yadana gas field, offshore Myanmar. Mar. Petrol. Geol. 109, 589–606. https://doi.org/10.1016/j.marpetgeo.2019.06.044.

Tian, W.C., Lu, S.F., Huang, W.B., Wang, S.P., Gao, Y., Wang, W.M., Li, J.B., Xu, J.P., Zhan, Z.C., 2019. Study on the full-range pore size distribution and the movable oil distribution in glutenite. Energy Fuels 33, 7028–7042. https://doi.org/10.1021/acs.energyfuels.9b00999.

Wang, J., Cao, Y.C., Liu, K.Y., Costanzo, A., Feely, M., 2018. Diagenesis and evolution of the lower Eocene red-bed sandstone reservoirs in the Dongying Depression, China. Mar. Petrol. Geol. 94, 230–245. https://doi.org/10.1016/j.marpetgeo.2018.04.011.

Wang, Q.C., Chen, D.X., Gao, X.Z., Wang, F.W., Li, J.H., Liao, W.H., Wang, Z.Y., Xie, G.J., 2020. Microscopic pore structures of tight sandstone reservoirs and their diagenetic controls: a case study of the Upper Triassic Xujiahe Formation of the Western Sichuan Depression, China. Mar. Petrol. Geol. 113, 104119. https://doi.org/10.1016/j.marpetgeo.2019.104119.

Wang, D.D., Dong, Q.S., Zhang, J.D., Zhou, X.G., Zhang, W.H., Liu, W.B., 2020. New views of tectonic evolution in the Tonghua, Liuhe and Hongmiaozi residual faulted basins, Northeast China. China Geol. 3, 501–503. https://doi.org/10.31035/cg2020034.

Wang, Y.S., Gao, Y., Fang, Z.W., 2021. Pore throat structure and classification of Paleogene tight reservoirs in Jiyang depression, Bohai Bay Basin, China. Petrol. Explor. Dev. 48, 308–322. https://doi.org/10.1016/S1876-3804(21)60025-3.

Wang, Z.Y., Lv, K.L., Wang, G.H., Deng, K.J., Tang, D.G., 2010. Study on the shape control and photocatalytic activity of high-energy anatase titania. Appl. Catal. B Environ. 100, 378–385. https://doi.org/10.1016/j.apcatb.2010.08.014.

Xi, K.L., Cao, Y.C., Jahren, J., Zhu, R.K., Bjørlykke, K., Haile, B.G., Zheng, L.J., Hellevang, H., 2015a. Diagenesis and reservoir quality of the lower Cretaceous Quantou formation tight sandstones in the southern Songliao Basin, China. Sediment. Geol. 330, 90–107. https://doi.org/10.1016/j.sedgeo.2015.10.007.

Xi, K.L., Cao, Y.C., Wang, Y.Z., Girma, H.B., Zhang, X.X., Zhang, J.H., Jin, J.H., 2015b. Diagenesis and porosity-permeability evolution of low permeability reservoirs: a case study of Jurassic Sangonghe Formation in Block 1, central Junggar Basin, NW China. Petrol. Explor. Dev. 42, 475–485. https://doi.org/10.1016/S1876-3804(15)30040-9.

Xiao, D.S., Lu, Z.Y., Jiang, S., Lu, S.F., 2016. Comparison and integration of experimental methods to characterize the full-range pore features of tight gas sandstone—a case study in Songliao Basin of China. J. Nat. Gas Sci. Eng. 34, 1412–1421. https://doi.org/10.1016/j.jngse.2016.08.029.

Xu, S.X., Dong, Q.S., Lou, R.X., Li, S.Z., Wang, D.D., Zhang, W.H., 2019. Sedimentary characteristics and oil-gas exploration prospect of Liuhe Basin, Jilin. Global Geol. 38, 215–224 (**in Chinese**).

Zhang, H., Lu, S.F., Li, W.H., Tian, W.C., Hu, Y., He, T.H., Tan, Z.Z., 2017. Application of ΔLogR technology and BP neural network in organic evaluation in the complex lithology tight stratum. Prog. Geophys. 32, 1308–1313 (**in Chinese**).

Zhang, L.C., Lu, S.F., Xiao, D.S., Gu, M.W., 2017. Characterization of full pore size distribution and its significance to macroscopic physical parameters in tight glutenites. J. Nat. Gas Sci. Eng. 38, 434–449. https://doi.org/10.1016/j.jngse.2016.12.026.

Zhang, L.C., Xiao, D.S., Lu, S.F., Jiang, S., Chen, L., Guo, T.L., Wu, L.Y., 2020. Pore development of the Lower Longmaxi shale in the southeastern Sichuan Basin and its adjacent areas: Insights from lithofacies identification and organic matter. Mar. Petrol. Geol. 122, 104662. https://doi.org/10.1016/j.marpetgeo.2020.104662.

Zhang, Y.C., Zeng, J.H., Dai, Z.X., Viswanathan, H., Xiao, T., Ma, Y., Feng, X., 2018. Experimental investigation on oil migration and accumulation in tight sandstones. J. Petrol. Sci. Eng. 160, 267–275. https://doi.org/10.1016/j.petrol.2017.10.049.

Zhao, W.B., Hu, S.Y., Deng, X.Q., Bai, B., Tao, S.Z., Sun, B., Wang, Q.R., Cheng, D.X., 2021. Physical property and hydrocarbon enrichment characteristics of tight oil reservoir in Chang 7 division of Yanchang Formation, Xin'anbian oilfield, Ordos Basin, China. Petrol. Sci. 18, 1294–1304. https://doi.org/10.1016/j.petsci.2020.07.001.

Zeng, L.B., Li, X.Y., 2009. Fracutres in sandstone reservoirs with ultra-low permeability: a case study of the upper Triassic Yanchang formation in the Ordos Basin, China. AAPG (Am. Assoc. Pet. Geol.) Bull. 93, 461–477.

Zou, C.N., Tao, S.Z., Bai, B., Yang, Z., Zhu, R.K., Hou, L.H., Yuan, X.J., Zhang, G.S., Wu, S.T., Pang, Z.L., Wang, L., 2015. Differences and relations between unconventional and conventional oil and gas. China Petrol. Explor. 20, 1–16 (**in Chinese**).

Zou, C.N., Tao, S.Z., Zhang, X.X., He, D.B., Zhou, C.M., Gao, X.H., 2009. Geologic characteristics, controlling factors and hydrocarbon accumulation mechanisms of China's Large Gas Provinces of low porosity and permeability. Sci. China Earth Sci. 52, 1068–1090. https://doi.org/10.1007/s11430-009-0104-1.